NORSAR

ROYAL NORWEGIAN COUNCIL FOR SCIENTIFIC AND INDUSTRIAL RESEARCH

NORSAR Scientific Report No. 1–86/87

SEMIANNUAL TECHNICAL SUMMARY

1 April – 30 September 1986

L.B. Loughran (ed.)

Kjeller, November 1986

VII. SUMMARY OF TECHNICAL REPORTS/PAPERS PREPARED

VII.1 Stability of various f-k estimation techniques

Experience with real-time NORESS processing has shown that estimates of phase velocity and azimuth of regional phases usually contain a fair amount of uncertainty. Thus, the median azimuth difference between P and Lg of the same event in RONAPP was found to be 5 degrees for a set of 132 Western Norway events (Mykkeltveit, 1985). In some cases, the difference exceeded 10 degrees, and although this performance is sufficiently good for phase association purposes, there is clearly a possibility of significant errors in locating the event under such circumstances.

Kværna and Doornbos (1986) described a method to estimate the slowness vector using arrays of either vertical or 3-component seismometers. They compared the performance of various algorithms (e.g., beamforming versus maximum likelihood, single frequency vs wide-band) for the P phases of a set of 5 events from approximately the same location (Leningrad region). Their conclusion was that conventional f-k processing of vertical sensor data provided more stable estimates than estimates obtained by similar processing of three-component arrays or sensors.

In this paper we pursue this investigation further, by concentrating on conventional f-k estimation (single frequency and wide band) for a suite of reference events of known origin. We have selected a set of 10 chemical explosions from a dam construction site (Blåsjø) in southern Norway:

Site coordinates:	59.31°N 6.95°E
True azimuth from NORESS:	240.19 degrees
Distance from NORESS:	301.2 km

The size of the explosions are typically 50 tons TNT. All of the events have a high SNR at NORESS; thus noise interference in the slowness vector estimates is minimal.

A list of the reference events is given in Table VII.1.1. An example of NORESS recordings (Event 1) produced by RONAPP is shown in Fig. VII.1.1. The spectra for P, S_n, Lg and the preceding noise are displayed in Fig. VII.1.2.

Fig. VII.1.3 shows the results of f-k analysis of the P_n phase for each of the 10 events. Four different methods have been chosen for frequency selection:

a) Narrow band - variable frequency

The frequency f_o selected for each event is the dominant frequency of the signal as determined by the cycle count method in RONAPP.

b) Broadband - variable frequency

Processing is done in the band $[f_o - f_o/4, f_o + f_o/4]$ where f_o is the dominant frequency.

c) Narrow band - 7.0 Hz

In this case the frequency has been kept fixed (f_o = 7.0 Hz) for all events.

d) Broadband 5.25 - 8.75 Hz

This is analogous to b) but with f_o = 7.0 Hz kept fixed for all events.

It is clear from the figure that by far the most stable result is obtained by method d). As seen in Table VII.1.2, the mean azimuth is

estimated at 242.19 deg, and the maximum spread around the mean is only ±1 degree.

We also conducted f-k processing of the S_n and Lg phases of the 10 events, using the fixed frequency band approach, i.e., corresponding to c) and d). Fig. VII.1.4 shows the results for the single frequency case (4 Hz), plotted together with the P_n results from c) above. We notice that the azimuth spread is larger for the two secondary phases. There is a clear distinction between the estimated phase velocities of the primary and secondary phases, and the S_n phase velocities tend to be larger than those of Lg.

In Fig. VII.1.5, a similar plot is presented corresponding to the broadband, fixed frequency approach (cf. d) above). We now see a clear phase velocity separation among all three phase types. In addition, estimated azimuths are generally consistent, although the scatter is somewhat larger for S_n and Lg than for P_n. Table VII.1.3 gives the detailed results for estimating the slowness vectors of the S_n and Lg phases, corresponding to the broadband case.

We also conducted some experiments, changing slightly the windowing positioning used for the f-k analysis and also in assessing the effects of introducing elevation correction for the NORESS seismometers. These did not produce any significant changes in the overall results, and do not appear to be factors of critical importance.

In conclusion, the broadband f-k estimation approach clearly provides the most stable estimates of azimuths and apparent velocities based on the data and methods applied in this investigation. It is particularly encouraging that we were able to obtain consistent separation between the S_n and Lg phases, based on phase velocity measurements alone. It must be noted, however, that all of the events processed had high signal-to-noise ratios, and the performance of the method at low SNR

is at present more uncertain. It also appears that the fixed frequency band approach is preferable in processing and comparing a suite of events from the same general area. However, the "best" frequency band to process will be regionally dependent, and criteria for selecting such bands need to be further developed.

T. Kværna
F. Ringdal

References

Kværna, T. and D.J. Doornbos (1986): An integrated approach to slowness analysis with arrays and three-component stations. Semiann. Tech. Summary, 1 Apr - 30 Sep 1986, NORSAR Sci. Rep. No. 2-85/86, Kjeller, Norway

Mykkeltveit, S. (1985): Evaluation of NORESS real-time processing performance: Case study for 132 Western Norway/North Sea events, Final Technical Report, 1 Apr - 30 Sep 1985, NORSAR Sci. Rep. No. 1-85/86, Kjeller, Norway.

Event Name	Date	Origin time	SNR P-phase	Magnitude M_L
BL1	06/04/85	03.13.59	209.6	2.3
BL2	06/07/85	14.42.39	62.7	2.0
BL3	06/19/85	13.03.53	20.2	2.5
BL4	06/27/85	08.45.37	17.0	2.1
BL5	06/28/85	15.42.12	33.4	2.0
BL6	07/02/85	12.55.59	16.3	2.1
BL7	07/03/85	20.28.01	25.1	2.4
BL8	07/05/85	03.59.29	45.6	2.3
BL9	07/16/85	17.33.12	115.8	2.5
BL10	07/29/85	13.55.18	42.0	2.8

Table VII.1.1 List of events used in this study. The table specifies event date, origin time, signal-to-noise ratio of the P-phase as computed by RONAPP and local magnitude (M_L). All of the events are located near the Blåsjø site 59.3°N, 6.95°E.

Broad-band, Pn-phase without elevation correction

VELMEAN	AZMEAN	THETA	PROB	SA	SB	SXMEAN	SYMEAN
7.99	242.19	-3.42	0.95	0.005640	0.001879	-0.110649	-0.058369

Event	Phase	Start	Stop	Freq	Delta	Azimuth	Velocity	Pmax
BL1	P	29.5	32.5	7.0	1.75	241.55	8.2107	0.6201
BL2	P	29.5	32.5	7.0	1.75	241.70	8.0854	0.5999
BL3	P	29.7	32.7	7.0	1.75	243.35	7.9359	0.5988
BL4	P	29.0	32.0	7.0	1.75	242.65	7.9497	0.5611
BL5	P	29.4	32.4	7.0	1.75	241.43	8.0618	0.5713
BL6	P	28.6	31.6	7.0	1.75	242.46	7.9134	0.5770
BL7	P	29.1	32.1	7.0	1.75	242.78	7.7779	0.5539
BL8	P	29.0	32.0	7.0	1.75	242.11	8.0143	0.6006
BL9	P	29.0	32.0	7.0	1.75	242.13	7.9139	0.6007
BL10	P	29.5	32.5	7.0	1.75	241.65	8.1300	0.6561

Explanation of variables:

Velmean : Mean velocity of 10 events from Sxmean and Symean.
Azmean : Mean azimuth of 10 events from Sxmean and Symean.
Theta : Rotational angle of the confidence ellipse.
Prob : Probability limit of the confidence ellipse.
Sa : Semi-axis of confidence ellipse.
Sb : Semi-axis of confidence ellipse.
Sxmean : Mean value of Sx.
Symean : Mean value of Sy.

Event : Event number.

Phase : Phase (E-means elevation correction).
Start : Start of data interval after start of disk-file.
Stop : Stop of data interval after start of disk-file.
Freq : Center analysis frequency.
Delta : Half-bandwidth of frequency band.
Azimuth : Estimated azimuth.
Velocity: Estimated velocity.
Pmax : Normalized power of estimated slowness peak

Table VII.1.2 Estimation results for the Pn phase using the broad-band f-k method with a fixed frequency band.

Broad-band, Sn-phase without elevation correction

VELMEAN	AZMEAN	THETA	PROB	SA	SB	SXMEAN	SYMEAN
4.71	238.35	-41.57	0.95	0.023276	0.004850	-0.180698	-0.111388

Event	Phase	Start	Stop	Freq	Delta	Azimuth	Velocity	Pmax
BL1	S	63.0	66.0	4.0	1.00	239.25	4.7096	0.3302
BL2	S	63.0	66.0	4.0	1.00	239.38	4.6098	0.4635
BL3	S	63.2	66.2	4.0	1.00	240.89	4.6896	0.4960
BL4	S	62.5	65.5	4.0	1.00	237.74	4.7903	0.4719
BL5	S	62.9	65.9	4.0	1.00	239.75	4.6864	0.4632
BL6	S	62.1	65.1	4.0	1.00	236.02	4.7033	0.3768
BL7	S	62.6	65.6	4.0	1.00	239.43	4.6683	0.4710
BL8	S	62.5	65.5	4.0	1.00	235.38	4.8004	0.4906
BL9	S	62.5	65.5	4.0	1.00	241.46	4.6534	0.4938
BL10	S	63.0	66.0	4.0	1.00	233.92	4.8209	0.4538

Part 1

Broad-band, Lg-phase without elevation correction

VELMEAN	AZMEAN	THETA	PROB	SA	SB	SXMEAN	SYMEAN
3.96	238.86	-26.01	0.95	0.013890	0.004894	-0.216135	-0.130595

Event	Phase	Start	Stop	Freq	Delta	Azimuth	Velocity	Pmax
BL1	LG	69.0	72.0	4.0	1.00	240.73	3.9287	0.5114
BL2	LG	69.0	72.0	4.0	1.00	239.15	3.9551	0.5657
BL3	LG	69.2	72.2	4.0	1.00	240.47	3.8741	0.5300
BL4	LG	68.5	71.5	4.0	1.00	238.19	3.9711	0.6067
BL5	LG	68.9	71.9	4.0	1.00	238.06	4.0199	0.5901
BL6	LG	68.1	71.1	4.0	1.00	237.03	4.0670	0.5250
BL7	LG	68.6	71.6	4.0	1.00	238.45	3.9672	0.5610
BL8	LG	68.5	71.5	4.0	1.00	238.73	3.9348	0.5509
BL9	LG	68.5	71.5	4.0	1.00	239.20	4.0127	0.5987
BL10	LG	69.0	72.0	4.0	1.00	238.47	3.9202	0.5215

Part 2

Table VII.1.3 **Estimation results as in Table VII.1.2, but corresponding to the Sn phase (Part 1) and the Lg phase (Part 2).**

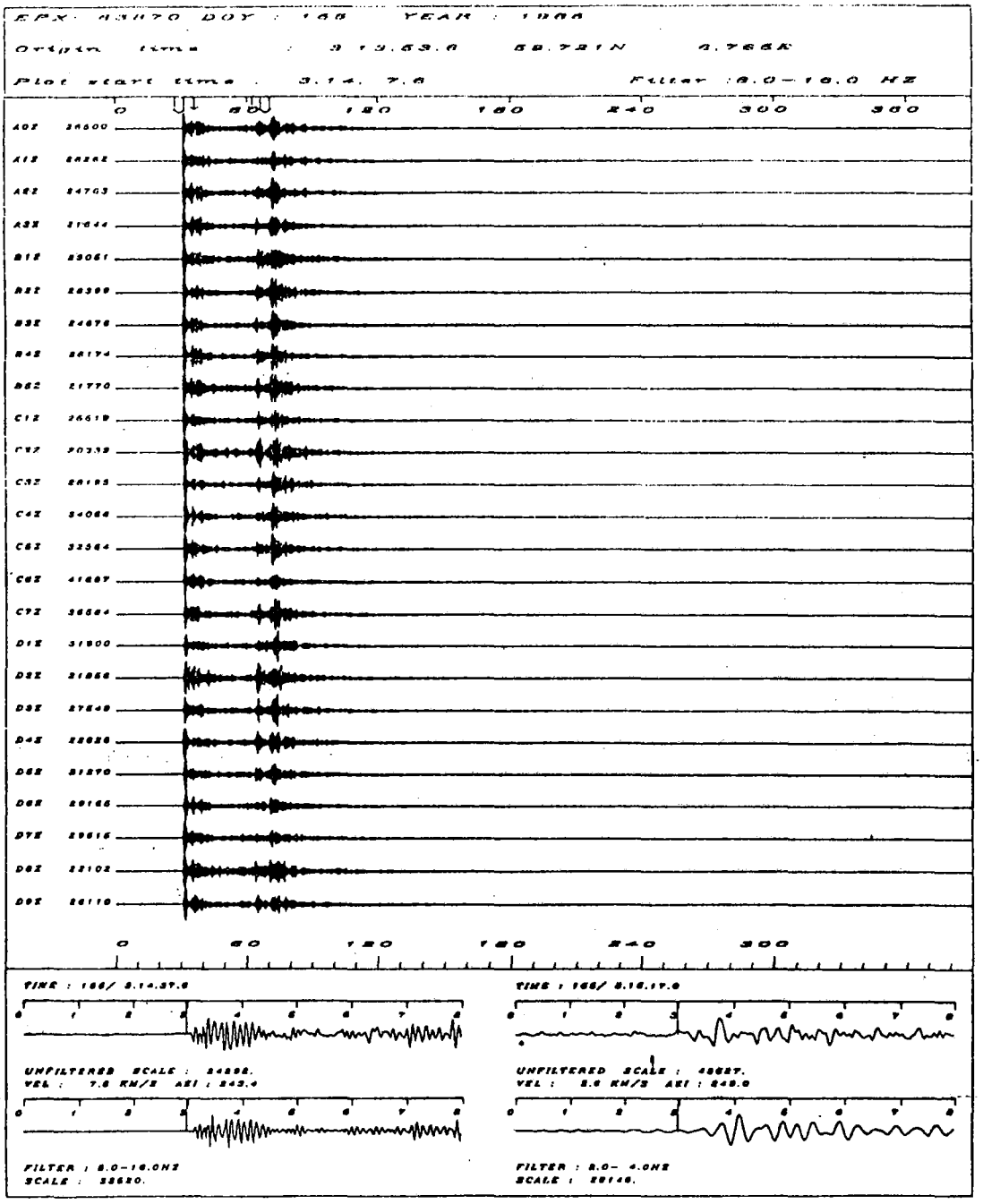

Fig. VII.1.1 NORESS waveform plots for Event 1 of Table VII.1.1. The large arrows mark the onsets of P and Lg, respectively. At the bottom, the P and Lg beams are shown in an expanded scale. Note the difference in frequency contents of the two phases.

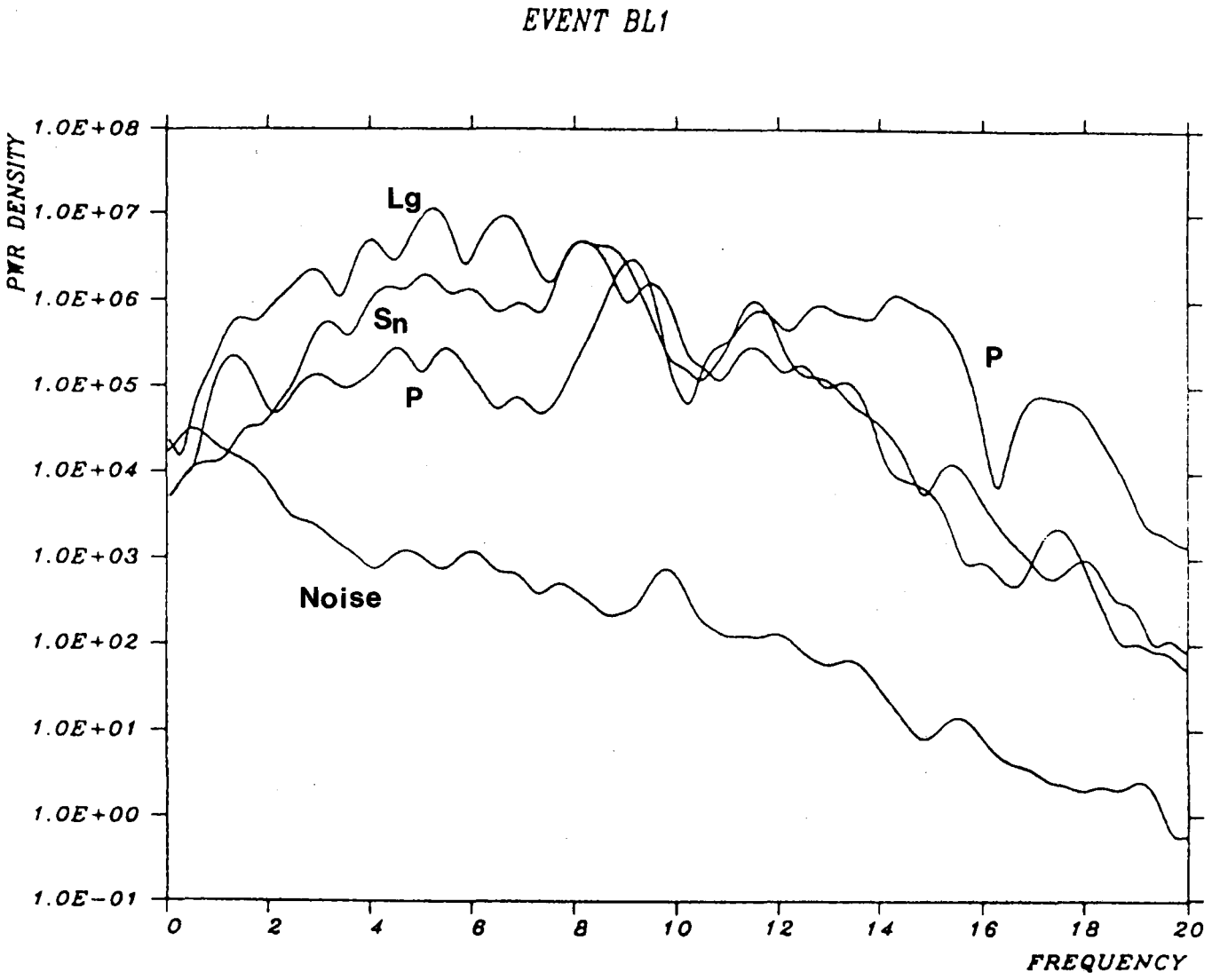

Fig. VII.1.2 Power density spectra of the P, S_n and Lg phases of Event 1, as recorded by NORESS instrument AOZ. The noise spectrum prior to P is also shown.

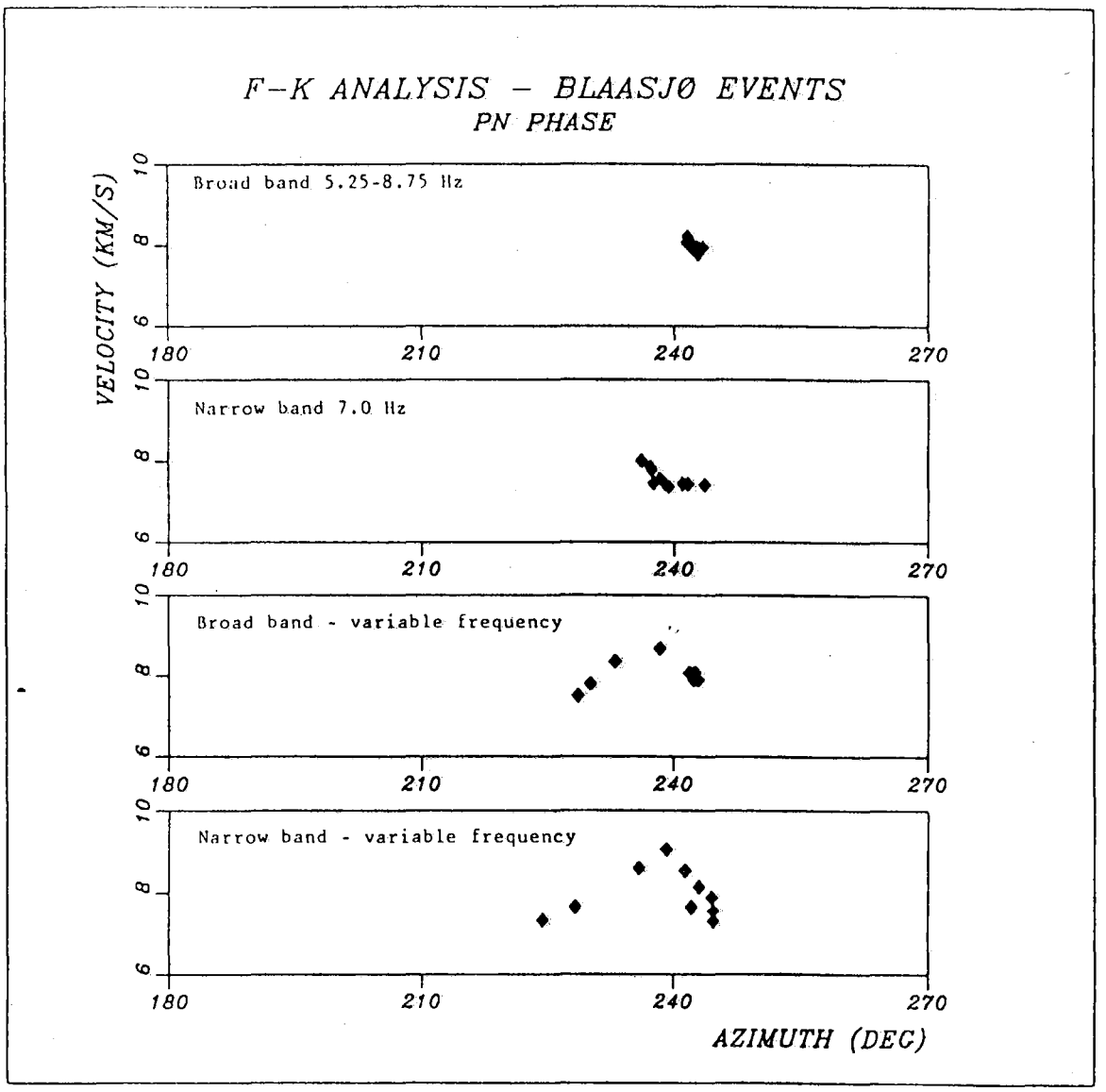

Fig. VII.1.3 Processing results (azimuth and phase velocity) for the Pn phase of the 10 events in the data base. Results using four different approaches, as described in the text, are shown. Note the excellent consistency of the results for the broadband case shown on top.

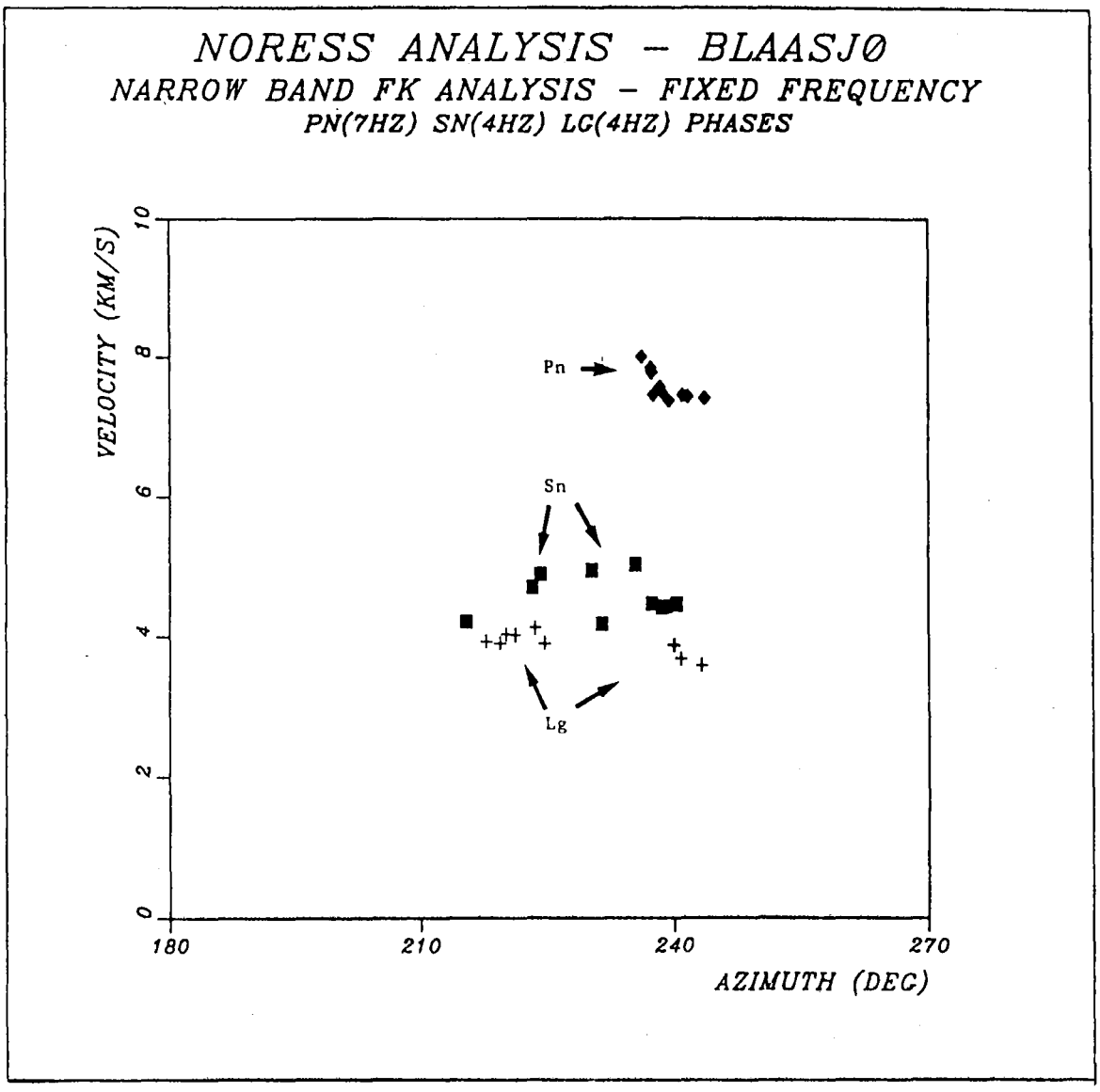

Fig. VII.1.4 Results using monochromatic f-k analysis of Pn, Sn and Lg phases of the 10 events. The processing frequency has been kept fixed for all events, but is higher (7 Hz) for Pn than for Sn and Lg (4 Hz).

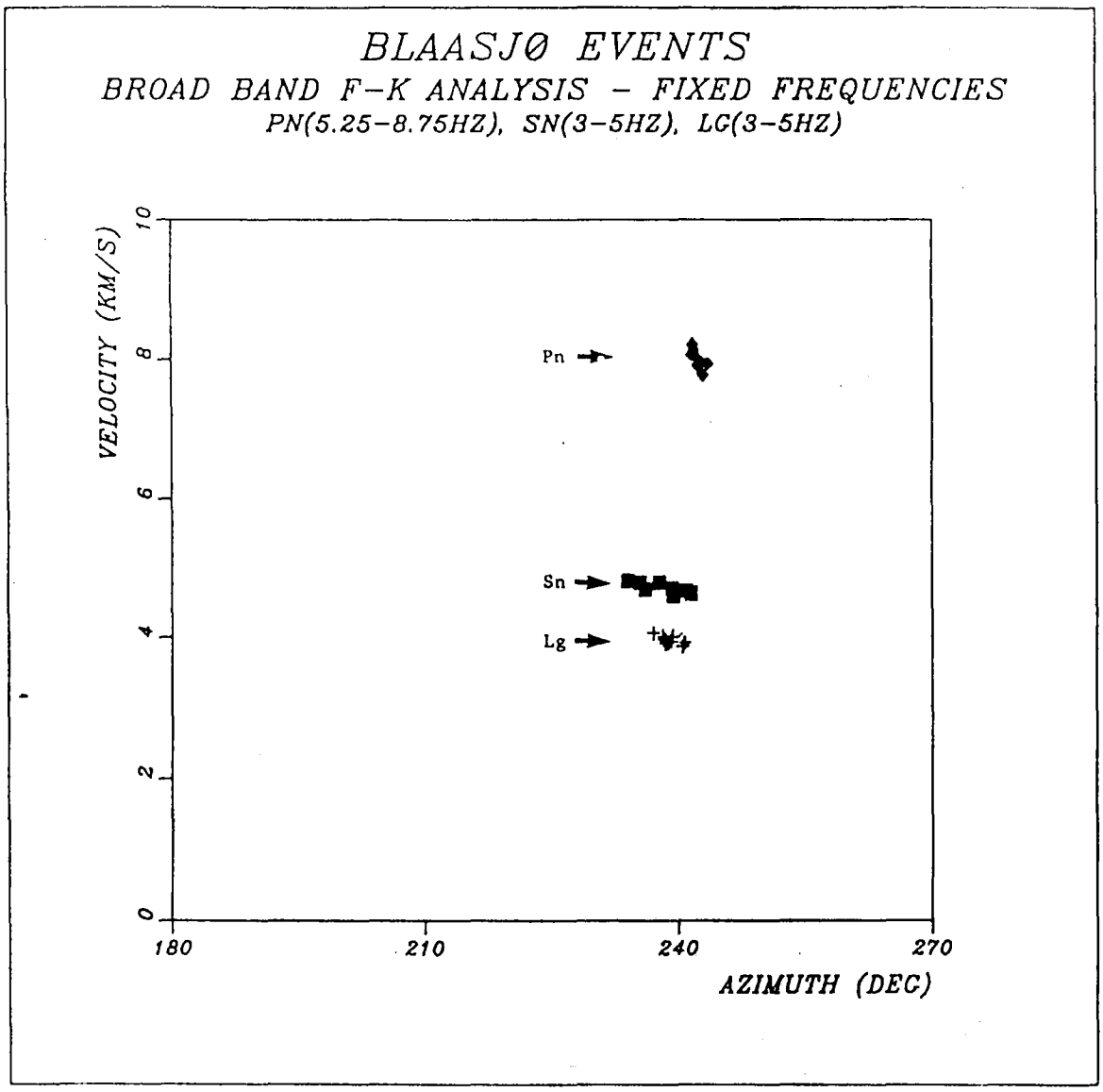

Fig. VII.1.5 Results using broadband f-k analysis of Pn, Sn and Lg phases of the 10 events. The processing frequencies have been kept fixed, as indicated in the plot. Note in particular that there is a clear phase velocity separation between each of the three phase types.